



HAL
open science

Modelling and Preliminary Studies for a Self-Reacting Point Absorber WEC

Sébastien Olaya, Jean-Matthieu Bourgeot, Mohamed Benbouzid

► **To cite this version:**

Sébastien Olaya, Jean-Matthieu Bourgeot, Mohamed Benbouzid. Modelling and Preliminary Studies for a Self-Reacting Point Absorber WEC. IEEE ICGE 2014, Mar 2014, Sfax, Tunisia. pp.14-19. hal-01063616

HAL Id: hal-01063616

<https://hal.science/hal-01063616v1>

Submitted on 12 Sep 2014

HAL is a multi-disciplinary open access archive for the deposit and dissemination of scientific research documents, whether they are published or not. The documents may come from teaching and research institutions in France or abroad, or from public or private research centers.

L'archive ouverte pluridisciplinaire **HAL**, est destinée au dépôt et à la diffusion de documents scientifiques de niveau recherche, publiés ou non, émanant des établissements d'enseignement et de recherche français ou étrangers, des laboratoires publics ou privés.

Modelling and Preliminary Studies for a Self-Reacting Point Absorber WEC

Sébastien Olaya
ENIB
EA 4325 LBMS
olaya@enib.fr

Jean-Matthieu Bourgeot
ENIB
EA 4325 LBMS
bourgeot@enib.fr

Mohamed Benbouzid
University of Brest
EA 4325 LBMS
Mohamed.Benbouzid@univ-brest.fr

Abstract—This paper deals with the special case modelling, in both frequency and time domain, of a self-reacting wave energy converter where the reaction force is obtained using a damping plate. In order to take into account the viscous damping that arises on the plate due to the flow separation at the sharp corners, an additional non-linear term have to be introduce. The influence of this non-linearity is then evaluate in a qualitative manner and obviously it is found that we can not neglect it.

Index Terms—Wave energy converter, state-space model, phenomenologically one-body equivalent model

NOMENCLATURE

\bar{P}	Average extracted power	[kW]
\ddot{z}_i	Vertical acceleration of body i	[m/s ²]
\dot{z}_i	Vertical velocity of body i	[m/s]
η	Wave surface elevation	[m]
κ_i	Buoyancy stiffness of body i	[N/m]
ρ	Density of sea water	[kg/m ³]
b_L	Generator load damping	[N.s/m]
b_{drag}	Additional equivalent drag damping	[N.s/m]
b_{ij}	Radiation damping	[N.s/m]
C_d	Drag coefficient	[without unit]
D_b	Buoy outer diameter	[m]
d_b	Buoy draft	[m]
D_p	Plate diameter	[m]
D_s	Spar diameter	[m]
d_s	Spar draft	[m]
f_{drag}	Drag force applied on the plate	[N]
$f_{ex,i}$	Wave excitation force on body i	[N]
g	Acceleration of gravity	[m/s ²]
h	Water depth	[m]
h_p	Plate height	[m]
m_i	Mass of the body i	[kg]
$m_{a,ij}$	Added mass	[kg]
S_p	Cross sectional area of the plate	[m ²]
z_i	Vertical displacement of body i	[m]
PTO	Power Take-Off	
RAO	Response Amplitude Operator	
WEC	Wave Energy Converter	

I. INTRODUCTION

This paper is about the developpment of a new french wave energy converter referenced as the “EM Bilboquet” project (see Fig.1). The power take-off (PTO) extracts mechanical

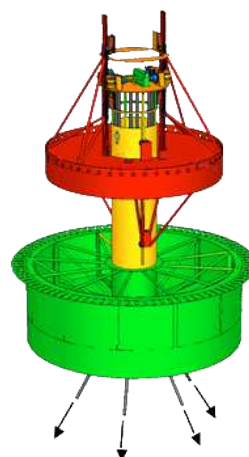


Fig. 1. Project “EM Bilboquet”.

power due to incoming waves by a system made up of a cylindrical buoy sliding along a partially submerged structure. This structure is made up of a vertical cylinder, referenced in the following as spar, with a damping plate attached at its keel. Energy resulting from the relative motion between the two concentric bodies is harnessed by rack-and-pinion which drives a permanent magnet synchronous generator through a gearbox. Wave energy converters using a reaction source which is not the seabed i.e. such as a plate, are referenced in the wave energy literature as self-reacting WEC and because horizontal dimensions of the buoy is small compared to the length of the incident wave, the term of self-reacting point absorber is used. The use of a submerged body acting as a reference for the floating body which can react against is not a new concept but will have a promising future.

In the following, section II presents the mathematical modelling necessary background for a generic two-body wave energy converter which reacts against a damping plate. In section III, we perform a frequency analysis including a non-linear term, modelling the vortex shedding phenomenon appearing due to the damping plate. Section IV is about time-dependent model where we show how to deal with the wave excitation force non-causality of a two-body WEC. Finally before concluding we give some numerical results for both frequency and time average power prediction in section V.

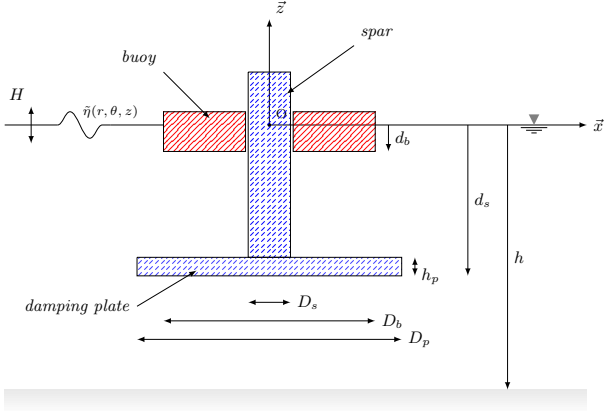


Fig. 2. Definition sketch of the wave energy converter.

II. MATHEMATICAL MODELLING

A. Background

In this section we present the mathematical formulation of the linearised model for a generic self-reacting WEC¹. For sake of simplicity, the total structure dynamics is restricted to the heaving mode. Under the assumption of linear wave potential theory, the linearised equations of motion in the heaving mode is given in an earthbound reference frame coordinating system with its origin O located at the intersection of the undisturbed free surface level with cylinders axes and the z-axis is positive upward (Fig. 2).

From the Newton's second law and using matrix notations² we have

$$M\ddot{\xi}(t) = \mathbf{F}(t) \quad (1)$$

where

- M is the body mass matrix where the diagonal elements m_1 and m_2 are respectively defined for the buoy and platform mass.
- $\xi = [z_1 \ z_2]^T$ is the vertical excursion with respect to the equilibrium position.
- \mathbf{F} is the generalised force vector which can be expressed in term of several components such as

$$\mathbf{F}(t) = \mathbf{F}_{ex}(t) + \mathbf{F}_r(t) + \mathbf{F}_s(t) + \mathbf{F}_L(t) + \mathbf{F}_{moor}(t) \quad (2)$$

where

- $\mathbf{F}_{ex} = [f_{ex,1} \ f_{ex,2}]^T$ is the wave excitation force. For body i , it can be expressed in the time-domain as

$$f_{ex,i}(t) = \int_{-\infty}^{\infty} h_{ex,i}(t - \tau)\eta(0, \tau)d\tau \quad (3)$$

with $\eta(0, \tau)$ the wave elevation at the origin O and $h_{ex,i}(t)$ is the impulse response of the wave excitation force [1] related to the geometry of the body i .

¹i.e. we do not make any assumption on the PTO principle.

²In term of notation, matrices are denoted by capital letters while vectors are in bold italic letters.

- \mathbf{F}_r is the force associated to the radiation problem. In linear potential theory it is conventional to decompose this force in two parts which are frequency dependent. One is proportional to the acceleration of body and the other is proportional to his velocity and are respectively referenced as added mass and radiation damping matrix

$$\mathbf{F}_r = -M_a\ddot{\xi}(t) - B\dot{\xi}(t) \quad (4)$$

where

$$M_a = \begin{bmatrix} m_{a,11} & m_{a,21} \\ m_{a,12} & m_{a,22} \end{bmatrix} \text{ and } B = \begin{bmatrix} b_{11} & b_{21} \\ b_{12} & b_{22} \end{bmatrix}$$

The off-diagonal elements in the matrice represent the hydrodynamic coupling term between buoy and platform. All those coefficients are frequency dependent.

- \mathbf{F}_s is the net restoring force due to gravity and buoyancy. It is proportional to the displacement of the body structure from its equilibrium position. The coefficient of proportionality is denoted K_s and is referenced as the buoyancy stiffness matrix

$$\mathbf{F}_s = -K_s\xi \quad (5)$$

where the diagonal elements are respectively defined for the buoy and the platform by κ_1 and κ_2 such as

$$\kappa_i = \rho g \iint_{S_{F0,i}} dS$$

with ρ the water density, g is the gravitational acceleration and $S_{F0,i}$ is the water plane area at equilibrium condition (see [2] for further details). Then for cylindrical shapes we have $\kappa_1 = \rho g \frac{\pi}{4} (D_b^2 - D_s^2)$ for the buoy and $\kappa_2 = \rho g \frac{\pi}{4} D_s^2$ for the spar.

- \mathbf{F}_L is the force due to the generator. In the remainder of this paper we will assume a passive loading such as

$$\mathbf{F}_L = -b_L u_r \quad (6)$$

where b_L is the generator damping³ and $u_r = (\dot{z}_1 - \dot{z}_2)$ is the relative velocity between the buoy and the platform.

- \mathbf{F}_{moor} is the force due to the mooring lines and can be represented by a restoring force or a non-linear force. In the following, we will not investigate this aspect. We suppose that the energy extraction in heaving mode is not or less-pertubated by this effort.

B. Hydrodynamic Coefficient Computation

Hydrodynamic parameters (i.e. added mass, radiation damping, and wave excitation force) are the starting point for modelling an offshore structure and are usually determinated using numerical software such as WAMIT which is based on the boundary integral equation method or more recently using CFD program. Due to the simplicity of the model geometry

³In this paper, we only investigate the passive loading case, because optimum control is out of the paper topic.

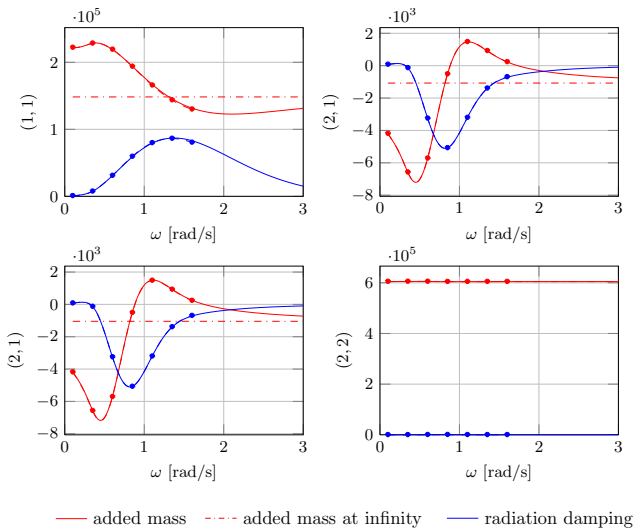


Fig. 3. Hydrodynamic coefficients (added mass and radiation damping) (dotted) based on a semi-analytical approach [5] and identified hydrodynamic coefficients (solid) obtained using MATLAB toolbox developed by Perez and Fossen [7].

and in view of model purposes (i.e. control and optimisation), an alternative to this approach is to use of a semi-analytical method. More explanations about the mathematical developments will be found in [2], [3], [4]. Regarding the specific structure depicted in Fig. 2 details will be found in [5] for the heaving mode. For confidential reasons, the real dimension of the “EM Bilboquet” project are not given. In the following numerical results are presented with the dimensions given in Table I and based on [6]. Added mass and radiation damping are given in Fig. 3. The infinite added mass have been obtained after we have identified a dynamic model using a tool presented in section IV. Wave excitation forces are shown in Fig. 4.

C. Additional Non-Linear Damping

Looking at the hydrodynamic coefficients at Fig. 3, we note the low value for the spar radiation damping which can be easily explain by its submergence depth. In order to enhance its modelling during the resonant oscillation and in view of its geometry i.e. a damping plate with sharp edges attached at the column bottom, we have to introduce an additional non-linear

TABLE I
GEOMETRIC INPUT PARAMETERS

Parameters	Symbol	Value	Units
Buoy draft	d_b	1.5	[m]
Buoy outer diameter	D_b	9.5	[m]
Plate diameter	D_p	11.8	[m]
Plate height	h_p	1.5	[m]
Spar diameter	D_s	3	[m]
Spar draft	d_s	35	[m]
Water depth	h	150	[m]

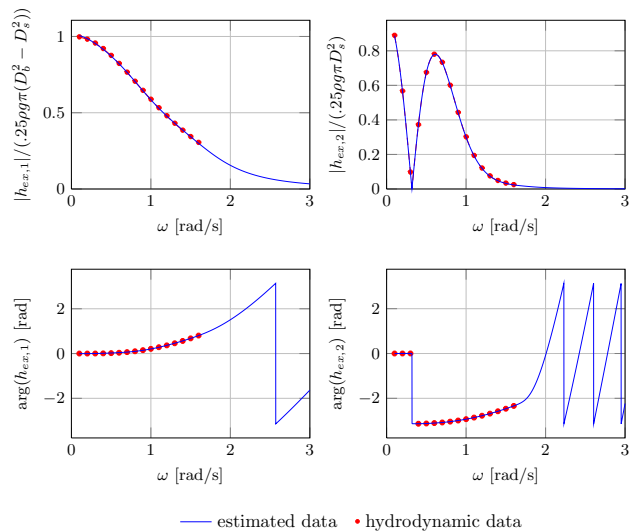


Fig. 4. Wave excitation forces (red dotted) and identified wave excitation forces (blue solid line).

drag force where the drag term is proportional to the square of the velocity and expressed as [8], [9], [10]

$$f_{drag} = -\frac{1}{2} \rho S_p C_d \dot{z}_2 |\dot{z}_2| \quad (7)$$

where S_p is the cross sectional area of the plate normal to the displacement, C_d is the drag coefficient. This coefficient have to be experimentally determined based on measure for different forcing amplitudes and frequencies. A better modelling would have been performed if rather than the drag plate velocity we have used the relative velocity between the fluid particle and the plate but at a cost of complexity increase.

III. FREQUENCY DOMAIN ANALYSIS

From body dynamic equation (1) and assuming sinusoidal oscillation such as $X(t) = \hat{X} e^{i\omega t}$, we have

$$Z_i(\omega) \hat{\xi} = \hat{F}_{ex}(\omega) + \hat{F}_L(\omega) + \hat{F}_{drag}(\omega) \quad (8)$$

where $Z_i(\omega)$ is the complex intrinsic mechanical impedance matrix which is related to the mechanical properties of the offshore structure [4, Chapter 5] and which is defined as

$$Z_i(\omega) = B(\omega) + i\omega[M + M_a(\omega) - \frac{K_s}{\omega^2}] \quad (9)$$

Also we added, as already explain in the previous section, an additional damping term ($F_{drag} = \begin{bmatrix} 0 & f_{drag} \end{bmatrix}^t$) in (8) modelling the drag force applied on the plate and for which in the frequency-domain, a linear function of the velocity such as $f_{drag} = -b_{drag} \dot{z}_2$ is choosen. Coefficient b_{drag} is determined based on a equivalent energy dissipation formulation of (7) during one cycle. So following this, we are looking for b_{drag} , for each ω , such as

$$b_{drag} \int_0^T \dot{z}_2^2(t) dt = \frac{1}{2} \rho S_p C_d \int_0^T |\dot{z}_2(t)| \dot{z}_2^2(t) dt \quad (10)$$

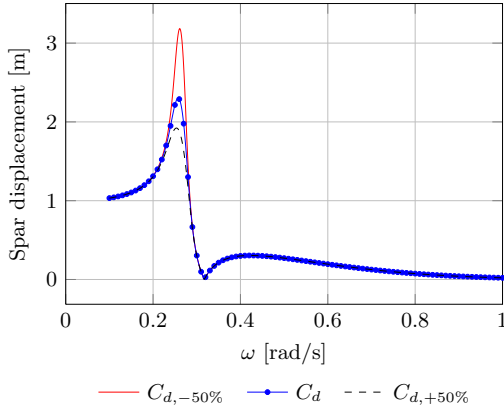


Fig. 5. Spar response amplitude operator for different values of the plate drag coefficient C_d and for a wave amplitude $A = 1\text{m}$.

After calculations, we find

$$b_{drag}(\omega) = \frac{1}{3}\omega\rho D_p^2 C_d |\hat{z}_2| = \alpha |\hat{z}_2| \quad (11)$$

where $\alpha = \frac{1}{3}\rho D_p^2 C_d$ and then we can re-write (8) such as

$$\begin{cases} \hat{f}_{ex,1} = z_{i,11}\hat{z}_1 + z_{i,12}\hat{z}_2 + b_L(\hat{z}_1 - \hat{z}_2) \\ \hat{f}_{ex,2} = z_{i,21}\hat{z}_1 + z_{i,22}\hat{z}_2 + \alpha|\hat{z}_2|\hat{z}_2 - b_L(\hat{z}_1 - \hat{z}_2) \end{cases} \quad (12)$$

This non-linear system can be solve using an iterative scheme.

$$\hat{z}_2^{(j)} = \frac{(f_{ex,2} - (z_{i,12} - b_L)\beta)}{z_{i,22} + b_L + \alpha|\hat{z}_2^{(j-1)}| - (z_{i,21} + b_L)\gamma} \quad (13)$$

where

$$\beta = \frac{\hat{f}_{ex,1}}{z_{i,11} + b_L} \quad \text{and} \quad \gamma = \frac{z_{i,12} - b_L}{z_{i,11} + b_L}$$

and

$$\hat{z}_1 = \beta - \gamma\hat{z}_2 \quad (14)$$

According to [2], the iterative scheme converges after few iterations. Figure 5 shows the spar response amplitude operator (RAO) for different values of the plate drag coefficient C_d (nominal and $\pm 50\%$) in the case where no generator damping is applied. Nominal value for the drag coefficient ($C_d = 1.17$) is based on [11][12] and have also been used by [10] in an optimisation context of the reacting body. It is important to note that, due to the non-linearity in amplitude in (12), frequency analysis can only be performed for regular waves at a given amplitude.

IV. TIME DOMAIN ANALYSIS

A. Approximated State-Space Cummins Formulation

According to [1] and more recently to [13] and [14], linear models based on the Cummins formulation [15] are a good starting point for modelling the response of a marine structure in waves. Cummins formulation is an integro-differential equation which relates the motion of the marine structure to the incoming wave.

Regarding the radiation force, Cummins shown that it can be approximated by the following representation in the time domain for the case of zero forward speed

$$\mathbf{F}_r(t) = -M_{a,\infty}\ddot{\boldsymbol{\xi}}(t) - \int_0^t \mathbf{K}(t-\tau)\dot{\boldsymbol{\xi}}(\tau)d\tau \quad (15)$$

where $M_{a,\infty}$ is the infinite-frequency added mass matrix defined as

$$M_{a,\infty} = \lim_{\omega \rightarrow \infty} M_a(\omega) \quad (16)$$

The second terms of the right-hand side is referenced as the fluid memory effect and capture energy transfert from the motion of the structure to the radiated waves. It can be relates to the frequency radiation damping such as

$$\mathbf{K}(t) = \frac{2}{\pi} \int_0^\infty \mathbf{B}(\omega)\cos(\omega t)d\omega \quad (17)$$

By replacing and combining terms in (1) by (5), (15) we obtain the Cummins formulation

$$(\mathbf{M} + M_{a,\infty})\ddot{\boldsymbol{\xi}}(t) + \int_0^t \mathbf{K}(t-\tau)\dot{\boldsymbol{\xi}}(\tau)d\tau + \mathbf{K}_s\boldsymbol{\xi}(t) = \mathbf{F}_{ext}(t) \quad (18)$$

where

$$\mathbf{F}_{ext}(t) = \mathbf{F}_{ex}(t) + \mathbf{F}_L(t) + \mathbf{F}_{drag}(t)$$

The main drawback of this formulation comes from numerical implementation of the convolution kernel in (3). Direct computation based on a discret-time approximation of the convolution terms requires to save enough past data to evaluate the integral at each simulation step. This approach can be time consuming in simulations and may require significant amounts of computer memory. A solution to overcome this problem is the use of parametric models based on a state-space representation that approximate the convolution kernels. Such techniques have been widely treated in the litterature and several identification schemes have been investigated either in time-domain or in frequency-domain. Authors in [13] and [16] provide a review of different methods in both domains. In a recent work [14], it has been highlighted that the use of frequency-domain methods have to be privileged due to their ‘‘superiority’’ in terms of accuracy and ease of estimation algorithm implementation. The same authors provide a MATLAB toolbox [7] which approximate the convolution terms of (15) by a linear time-invariant system such as (19) based on the modified Levi’s identification algorithm [17].

$$\int_0^t \mathbf{K}(t-\tau)\dot{\boldsymbol{\xi}}(\tau)d\tau \simeq \begin{cases} \dot{\mathbf{x}}(t) = \tilde{\mathbf{A}}_r\mathbf{x}(t) + \tilde{\mathbf{B}}_r\dot{\boldsymbol{\xi}}(t) \\ \tilde{\boldsymbol{\mu}}(t) = \tilde{\mathbf{C}}_r\mathbf{x}(t) \end{cases} \quad (19)$$

$\tilde{\mathbf{A}}_r$, $\tilde{\mathbf{B}}_r$, and $\tilde{\mathbf{C}}_r$ matrix are constants and approximate the convolution kernel (or impulse response) matrix $\mathbf{K}(t)$.

B. Approximated State-Space Model for the Wave Excitation Force

Regarding numerical implementation of the wave excitation forces, a similar procedure as the one above-explained is applied. However Falnes (1995), in [18], shown that the convolution kernel $h_{ex,i}(t)$ of (3) is not necessary causal because of

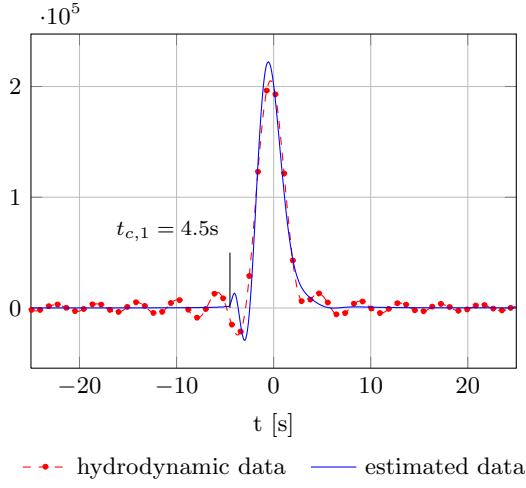


Fig. 6. Impulse response and causalizing time-shift for wave excitation force applied on the buoy.

the mathematical assumptions made for the hydrodynamic parameter determination. Because the wave elevation function $\eta(t)$ is necessary causal, (3) can be re-written as

$$f_{ex,i}(t) = \int_0^{t+t_{c,i}} h_{ex,i}(t-\tau)\eta(0,\tau)d\tau \quad (20)$$

where $t_{c,i}$ is the time of non-causality ($h_{ex,i} \simeq 0$ for $t < -t_{c,i}$) that shows that we have to know the futur value of $\eta(t)$. Then following [1] we are looking for an approximated state-space representation such as

$$\begin{aligned} \dot{\mathbf{x}}_i(t) &= \tilde{A}_{s,i}\mathbf{x}_i(t) + \tilde{B}_{s,i}\eta(0,t+t_{c,i}) \\ \tilde{f}_{ex,i}(t) &= \tilde{C}_{s,i}\mathbf{x}_i(t) \end{aligned} \quad (21)$$

where $\tilde{f}_{ex,i}(t)$ is the causal wave excitation force applied on body i . $\eta(0,t+t_{c,i})$ is the futur value of the free surface elevation at the origin O that must see body i in order to make wave excitation force causal. In the case of a single body, numerical implementation is straightforward using a simple delay applied between the causal wave excitation force and the free surface elevation. In facts, this corresponds to change the time reference which is no more referenced at the free surface elevation but now at the wave excitation force which is actually applied at instant t . In the case of a two-body system, we use the same idea but we have to choose between two causalizing times, which are not necessary the same. So considering body with the highest causalizing time-shift $t_{c,Max} = \max(t_{c,i})$ as the new reference, it follows that η have to be delayed with $t_{c,Max}$ and the wave excitation applied on the second body have to be delayed of $t_c = t_{c,Max} - \min(t_{c,i})$.

In Figure 6 and 7 we show the impulse responses based on computed hydrodynamic data and identified model respectively for the buoy and the spar. One can note the oscillations of the impulse response for the buoy due to the upper frequency limit of the hydrodynamic data (Fig. 4). In Figure 8 we give a block-diagram representation for the state-space approximated Cummins model.

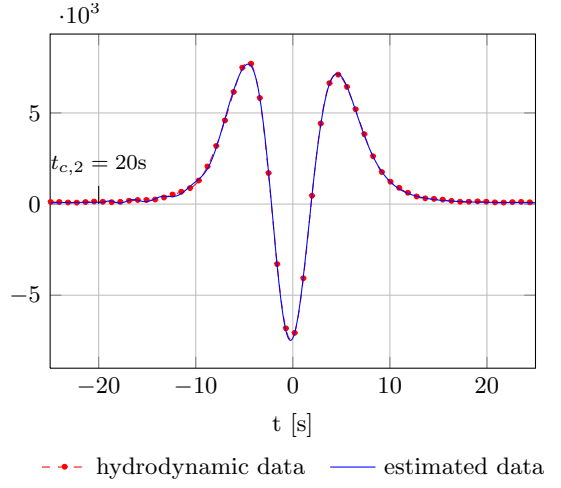


Fig. 7. Impulse response and causalizing time-shift for wave excitation force applied on the platform.

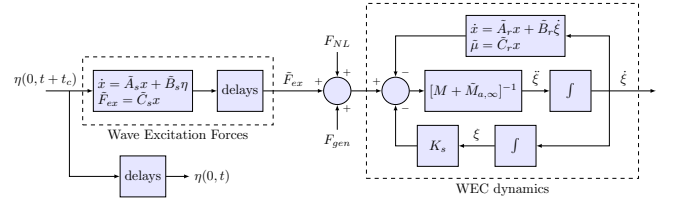


Fig. 8. Block diagram representation for state-space approximated Cummins model.

V. ON THE NON-LINEARITY TERM INFLUENCE

The main purpose of this section is to discuss, in a qualitative manner, the influence of the non-linearity due to the viscous damping. Based on linear assumptions, frequency analysis provide useful informations such as power prediction for both regular and irregular waves. However, due to the non-linearity in the model, we have to evaluate how much the linear principle is transgressed in order to know if linear assumptions are still valid. Mean extracted powers are presented, both in frequency- and time-domain (respectively denoted as FD and TD), in Table II, for regular wave of different amplitudes $A = \{0.5; 1; 2\}$ at the coupled structure resonance frequency $\omega = 0.75\text{rad/s}$ and for three different generator loadings without taking into account constraint limits. Resonance frequency have been obtained using modal analysis for an infinite generator load damping. Analysing the relative error, a good correlation is found between the two approaches. Based on linear assumptions, we know that the average power, for a given frequency, is related to the square wave amplitude such as $\bar{P}_{L,A_i} = \bar{P}_{A_1} A_i^2$ where, in our case, \bar{P}_{A_1} is the reference average power determined for $A = 1$ in the non-linear case. So based on this relation we can evaluate the relative error defined as $\epsilon_i, \% = 100 * (\bar{P}_{A_i} - \bar{P}_{L,A_i}) / \bar{P}_{A_i}$ between non-linear and linear assumption. Numericals results, based on time domain model, are given in Table III. Obviously, it is clear that non-linearity has a real influence on the power prediction and

TABLE II
AVERAGE POWER BASED ON NON-LINEAR ASSUMPTION

	$b_L = 1.10^6$			$b_L = 1.6.10^6$			$b_L = 2.10^6$		
	<i>TD</i>	<i>FD</i>	$\epsilon\%$	<i>TD</i>	<i>FD</i>	$\epsilon\%$	<i>TD</i>	<i>FD</i>	$\epsilon\%$
$\bar{P}_{A_{.5}}$	42.7	42.6	.2	55	54.9	.2	59.4	59.2	.3
\bar{P}_{A_1}	157.3	156.9	.2	188.4	187.4	.5	194.9	194.1	.4
\bar{P}_{A_2}	547.8	546.3	.3	600	598	.3	593.8	591.5	.4

TABLE III
COMPARAISON BETWEEN LINEAR AND NON-LINEAR ASSUMPTION

	$b_L = 1.10^6$	$b_L = 1.6.10^6$	$b_L = 2.10^6$
$\bar{P}_{L,A_{.5}} = \bar{P}_{A_1} A_{.5}^2$	39.3	47.1	48.7
$\epsilon_{.5,\%}$	7.96	14.36	18
$\bar{P}_{L,A_2} = \bar{P}_{A_1} A_2^2$	629.2	753.6	779.6
$\epsilon_{2,\%}$	14.86	25.6	31.28

moreover when we have a high generator load damping. In fact, when increasing the generator load damping, the stiffness between the buoy and the spar increases and therefore the spar starts to follow the buoy displacement leading to an increase of the energy losses (energy dissipation in the viscous term). According to this fact, it is reasonable to consider that the energy losses will considerably increase when working around the resonance i.e. at normal operating conditions. This is confirm looking at the Fig. 9 where we show the relative error for two different wave amplitudes when optimal passive loading control is applied.

VI. CONCLUSION

This paper deals with the special case modelling of a self reacting wave energy converter where reaction force is obtained using a damping plate. In order to take into account the viscous damping that arises on the plate, due to the flow separation at the sharp corners, non-linear term have to be included. A numerical study has been performed for regular waves with both frequency- and time-domain approaches. In this context, good correlations were found between them. Moreover and

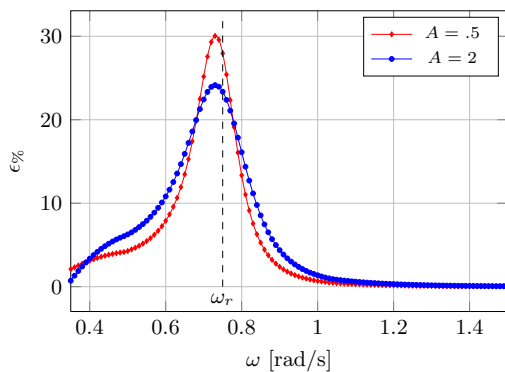


Fig. 9. Relative error between frequency model based on linear and non-linear assumptions for optimal passive loading.

based on a qualitative analysis, it has been shown that the non-linearity effect is not negligible, in particular when the wave energy converter is working at the resonance (normal operating conditions). This means that for some WECs, linear theory-based analysis and control are no longer valid. In the control context, optimal control is still an open problem.

VII. ACKNOWLEDGMENT

This work was founded in part by the Fonds Unique Interministériel (France) — "Project EM Bilboquet", in part by Région Bretagne, and in part by Conseil Général du Finistère.

REFERENCES

- [1] Z. Yu and J. Falnes, "State-space modelling of a vertical cylinder in heave," *Applied Ocean Research*, vol. 17, no. 5, pp. 265–275, 1995.
- [2] B. Molin, *Hydrodynamique des structures offshore - Guides pratiques sur les ouvrages en mer*, in French. Technip, 2002.
- [3] C. Linton and P. McIver, *Handbook of Mathematical Techniques for Wave/Structure Interactions*, 1st ed. Chapman and Hall/CRC, 2001.
- [4] J. Falnes, *Ocean Waves and Oscillating Systems - Linear Interactions Including Wave-Energy Extraction*. Cambridge University Press, Apr. 2002.
- [5] S. Olaya, J.-M. Bourgeot, and M. Benbouzid, "Hydrodynamic Coefficients and Wave Loads for a WEC Device in Heaving Mode," in *Proceedings of the 2013 MTS/IEEE OCEANS*, Bergen (Norway), Jun. 2013, pp. 1–6.
- [6] Ocean Power Technologies, "OPT PB150 PowerBuoy - Utility Power from Ocean Waves," pp. 0–1. [Online]. Available: <http://www.oceanpowertechnologies.com/pb150.html>
- [7] T. Perez and T. I. Fossen, "A Matlab Toolbox for Parametric Identification of Radiation-Force Models of Ships and Offshore Structures," *Modeling, Identification and Control: A Norwegian Research Bulletin*, vol. 30, no. 1, pp. 1–15, 2009.
- [8] H. Eidsmoen, "Simulation of a slack-moored heaving-buoy wave-energy converter with phase control," Norwegian University of Science and Technology, Trondheim, Norway, Tech. Rep., 1996.
- [9] L. Tao and S. Cai, "Heave motion suppression of a Spar with a heave plate," *Ocean Engineering*, vol. 31, no. 5, pp. 669–692, 2004.
- [10] S. Beatty and B. Buckham, "Sensitivity of point absorbing WECs to physical parameters of the reacting body," in *9th European Wave and Tidal Energy Conference (EWTEC)*, Southampton, UK, Sep. 2011, pp. 1–8.
- [11] F. M. White, *Fluid Mechanics, fourth edition*, 4th ed. McGraw-Hill Companies, 2002.
- [12] S. F. Hoerner, *Fluid-Dynamic Drag: Theoretical, Experimental and Statistical Information*. Hoerner Fluid Dynamics, 1965.
- [13] R. Taghipour, T. Perez, and T. Moan, "Hybrid frequency-time domain models for dynamic response analysis of marine structures," *Ocean Engineering*, vol. 35, no. 7, pp. 685–705, May 2008.
- [14] T. Perez and T. I. Fossen, "Practical aspects of frequency-domain identification of dynamic models of marine structures from hydrodynamic data," *Ocean Engineering*, vol. 38, no. 2-3, pp. 426–435, Feb. 2011.
- [15] W. Cummins, "The impulse response function and ship motion," Tech. Rep., 1962.
- [16] T. Perez and T. I. Fossen, "Time- vs. Frequency-domain Identification of Parametric Radiation Force Models for Marine Structures at Zero Speed," *Modeling, Identification and Control: A Norwegian Research Bulletin*, vol. 29, no. 1, pp. 1–19, 2008.
- [17] R. Pintelon, P. Guillaume, Y. Rolain, J. Schoukens, and H. Van Hamme, "Parametric identification of transfer functions in the frequency domain - a survey," *IEEE Trans. on Automatic Control*, vol. 39, no. 11, pp. 2245–2260, Nov. 1994.
- [18] J. Falnes, "On non-causal impulse response functions related to propagating water waves," *Applied Ocean Research*, vol. 17, no. 6, pp. 379–389, Dec. 1995.